Aerosol and Air Quality Research

ORIGINAL RESEARCH
https://doi.org/10.4209/aaqr.2020.07.0374

CO_2 Capture by Using a Membrane-absorption Hybrid Process in the Nature Gas Combined Cycle Power Plants

Wenfeng Dong*, Mengxiang Fang, Tao Wang, Fei Liu, Ningtong Yi

State Key Laboratory of Clean Energy Utilization, Zhejiang University, Hangzhou 310027, China

ABSTRACT

This study's main objective was to optimize the design parameters of the hybrid membrane-absorption CO_2-capture process in natural gas steam cycle (NGCC) power plants. To calculate the CO_2 concentration in the permeating gas and the required area for the separating membrane, a mass transfer model of a membrane for separating CO_2, N_2 and H_2O was developed in Aspen Plus. The effects of the CO_2 recovery rate of the membrane, the ratio of the feed gas pressure to the permeating-side gas pressure and the flow rate of the flue gas on the required area for the membrane, the power consumption of the compressor and the heat duty for the solvent regeneration were then analyzed. The optimal feed-gas-to-permeating-side-gas pressure ratio and the flue gas flow rate were found to be 10:1 and 50%, respectively. Furthermore, compared to traditional chemical absorption, the solvent regeneration's heat duty decreased by more than 20.7% when the gas flow rate and the CO_2 recovery rate were 100% and 20%, respectively.

Keywords: Membrane-absorption process, Mass transfer model, Natural gas steam combined cycle power plants, CO_2 capture, Monoethanolamine

1 INTRODUCTION

Carbon capture, utilization and storage (CCUS) technologies was mainly applied in the coal-fired field due to the carbon emission of coal-fired power plant was over twice for NGCC (natural gas steam cycle) power plants (Yu *et al.*, 2012). As a relatively clean energy, natural gas is widely used in various industrial fields. CO_2 reductions from NGCC power plants had a better application prospect in the long run. For an NGCC power plant with capacity of approximately 390–1600 MW_e, the carbon emissions from the flue gas was approximately 190–600 kg MW^{-1} (Martin-Gamboa *et al.*, 2018). Considering the considerable carbon emission of the NGCC power plant, CO_2 capture in the NGCC power plants will become a significance technical storage from a longer-term perspective, while CO_2 concentration of the flue gas in NGCC power plant was about 4 vol% due to high excess air ratio.

For the coal-fired power plant, the optimal regeneration duty of 30 wt% monoethanolamine (MEA) solution was about 3.6–4.5 GJ t-CO_2^{-1} with 80–90% of the CO_2 capture rate (Artanto *et al.*, 2012; Mangalapally *et al.*, 2012; von Harbou *et al.*, 2012; Rabensteiner *et al.*, 2014; Oh *et al.*, 2016). Therefore, high equipment disposable investment, solution regeneration duty and operating cost of CO_2 capture became the major obstacles of preventing large-scale adoption. Efforts of reducing carbon capture cost had been made on three major aspects: optimizing operational parameters, process modifications (Le *et al.*, 2011; Ahn *et al.*, 2013; Yang *et al.*, 2020) and developing better solvents (Yu *et al.*, 2019; Liu *et al.*, 2019; Yu *et al.*, 2020).

However, the power plant with the CO_2 capture process would result in reduction of power generation efficiency. Especially, CO_2 concentration of the flue gas in NGCC power plant (4 vol%) was much lower than that in coal-fired power plant (10–14 vol%). The driving force was relatively weak due to lower CO_2 concentration of the lower part of the absorber, which resulting high

OPEN ACCESS

Received: July 3, 2020
Revised: September 3, 2020
Accepted: September 3, 2020

* **Corresponding Author:**
wfdong@zju.edu.cn

Publisher:
Taiwan Association for Aerosol Research
ISSN: 1680-8584 print
ISSN: 2071-1409 online

solution flow and solution regeneration duty. The testing CO_2 partial pressure of flue gas was about 55 mbar, and the CO_2 capture rate was over 90%. When the structured packing 250.Y height over 12 m, the rich CO_2 loading was raised to 0.44 mol-CO_2 mol-MEA^{-1} MEA (Notz *et al.*, 2012; Agbonghae *et al.*, 2014). The optimal solution regeneration duty was about 3.7–4.2 GJ t-CO_2^{-1} (Li *et al.*, 2011; Mores *et al.*, 2014; Amann *et al.*, 2009; Luo *et al.*, 2015; Luo *et al.*, 2016), while the solution regeneration duty had a significant linear correlation with the effective mass transfer area, which was related to the specific surface area and height of the structured packing. The measured solution regeneration duty values were all over 7.0 GJ t-CO_2^{-1} when the CO_2 concentration was less than 5.5%. So, the practical solution regeneration duty was higher than the mentioned values above due to the lower rich CO_2 loading (Akram *et al.*, 2016).

To improve the driving force of the lower part of the absorber, Membrane Technology and Research (MTR) and the University of Texas at Austin previously proposed a hybrid system which considering amine scrubbing and membrane process (Freeman *et al.*, 2014). Maintaining the uniform overall CO_2 capture rate, CO_2 concentration of the flue gas could be enriched from 12% to 23% by using CO_2 enrichment membrane, and flue gas flow rate will be reduced to 47% accordingly. CO_2 concentration increased from 14% to 28%, which increasing the mass transfer driving force in the absorber (Frimpong *et al.*, 2019). CO_2 concentration in the flue gas was raised to 12 vol% with membrane unit in NGCC power plant. The total cost of the hybrid amine-membrane system was lowest when CO_2 concentration enriched to 12% (Ding *et al.*, 2017). The flue gas split ratio in the membrane unit was calculated by CHEMCAD, and absorber with a direct contact cooler (DCC) or pump-around, and variable lean loading was optimized in Aspen Plus. MATLAB software was also used to simulate the three-stage membrane process for CO_2 separation (Liu *et al.*, 2019). Few literature on mass transfer calculation model in Aspen Plus software. Few researchers concerned the simulation of the membrane-absorption hybrid process, while CHEMCAD and MATLAB software were just used for calculating the membrane process. CO_2 recovery rate and CO_2 concentration of membrane unit will affect the absorption process. So CHEMCAD and MATLAB software had no special advantages in calculating the overall performance of the hybrid process.

In this paper, the effect of CO_2 capture rate, specific surface area of structured packing, lean CO_2 loading and stripper pressure in the CO_2 capture process with 30 wt% MEA solution were studied. The mass transfer model of $CO_2/N_2/H_2O$ separation membrane was established based on the hybrid membrane-30-wt%-MEA process. Effect of CO_2 recovery rate of the membrane unit, operating pressure proportion of feed gas pressure over permeate gas pressure and flue gas flow ratio on membrane area, compressor power and solution regeneration duty were studied based on the membrane calculation model.

2 METHODS

The flow of the flue gas was about 21,600 Nm^3 h^{-1}, the CO_2 capture scale was 12,000 tons a^{-1}, and the annual operation time was 7500 h a^{-1} in the simulation. The CO_2 capture rate ranged from 50% to 90%. The specific components, pressure and temperature of the flue gas were shown in Table 1.

To improve the driving force of gas-liquid reaction in the lower part of the absorber, a portion of the flue gas was first pumped into the membrane separation unit. CO_2 concentration of the

Table 1. Base parameter of flue gas in the NGCC power plant.

Parameter	Unit	Value
Composition		
CO_2	vol%	4.20
O_2	vol%	5.00
N_2	vol%	81.77
H_2O	vol%	7.03
Pressure	bar	1.06
Temperature	°C	40

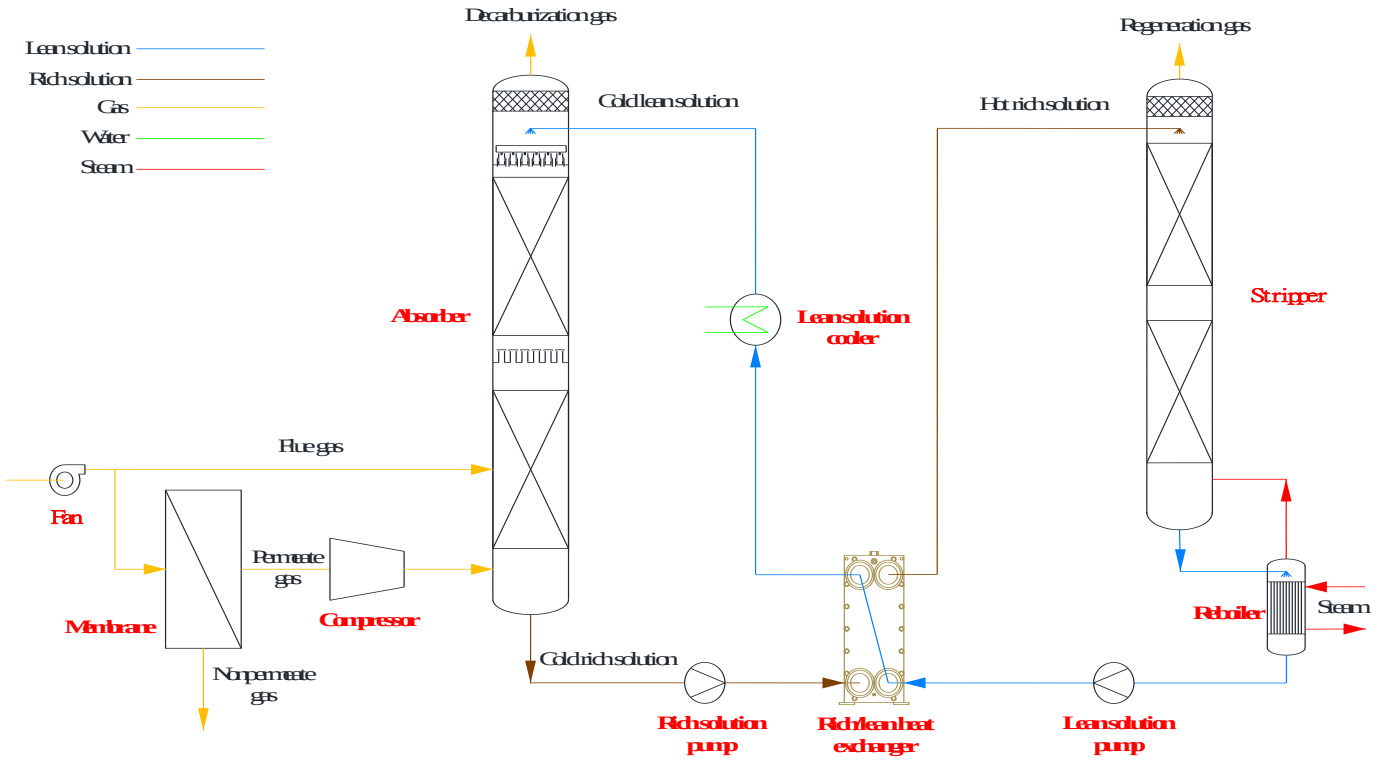

Fig. 1. Hybrid membrane-absorption CO_2 capture process in NGCC power plant.

flue gas was enriched to above 20 vol% in permeate gas, which could increase the rich CO_2 loading. This effect just worked in the lower part of the absorber, so the residual flue gas directly pumped into the upper part of the absorber, as shown in Fig. 1.

Aspen Plus software was applied in CO_2 capture process from the flue gas in the power plant with MEA solution. Rigorous physical and chemical properties were needed for evaluating the performance of the CO_2 capture process by using 30 wt% MEA solution. The electrolyte non-random two-liquid (e-NRTL) method and perturbed-chain statistical associating fluid theory (PC-SAFT) equation of state were used to compute liquid and vapor properties of the CO_2-MEA-H_2O system, respectively. The rate-based model of CO_2-MEA-H_2O system had been validated with pilot testing results. Based on the diffusion model, the hybrid membrane-absorption process of the CO_2 capture in NGCC power plant was built in Aspen Plus, as shown in Fig. 2. In order to reduce the compressor power of the hybrid process, the vacuum compressor was applied instead of compressor.

The composition of actual exhaust gas was complex, which will affect the performance of the absorption process. In order to simplify the simulation process, the following hypothesis was proposed: (1) The flue gas temperature was set as 40°C, and the ash and nitrogen sulfur oxides were ignored. (2) Degradation of solvent and corrosion of equipment were not considered in the simulation. (3) CO_2, O_2 and N_2 were selected as Henry gas, which conformed to Henry's law. (4) All heat and mass transfer equipment and process were set as heat insulation. 30 wt% MEA aqueous solution was selected as absorption solution. The temperature difference of the rich/lean solution heat exchanger between cold lean solution and cold rich solution was set as 5°C. Table 2 listed the diameter, packing type and model parameters of absorber and stripper. Bravo (1992) fitting equation was adopted to determine the effective mass transfer area of the structured packing in absorber and stripper.

The operating principle of the membrane unit was that different gas molecules had disparate permeation rates through membrane pores under a certain pressure difference. The permeability coefficient of gas in membrane structure was an important parameter, which directly affected the membrane area and CO_2 recovery rate. The calculation method of membrane area and CO_2 recovery rate were shown in Eqs. (1) and (2):

$$A_{mCO_2} = \frac{y_{CO_2P}U_P}{J_{CO_2}\left(\overline{xP - yP_{CO_2}}\right)} \quad (1)$$

$$\theta_{CO_2} = \frac{J_{CO_2}\left(\overline{xP - yP_{CO_2}}\right)A_{mCO_2}}{x_{CO_2F}U_F} \quad (2)$$

where A_{mCO_2} was the membrane area, m^2; θ_{CO_2} was the CO_2 recovery rate; x_{CO_2F} and y_{CO_2P} were the CO_2 concentration in feed and permeability gas, respectively; U_F and U_P were the total flow of feed and permeability gas, respectively, kmol h^{-1}; J_{CO_2} was the permeability coefficient, kmol h^{-1} m^{-2} kPa^{-1}; and $\overline{xP - yP_{CO_2}}$ was the CO_2 average differential pressure.

Recent years had seen great advances in membrane technology (Mubashir *et al.*, 2018). A membrane unit specifically developed by MTR for this application (Polaris™), with pure-gas CO_2 permeance values of 1000–2000 GPU (50 psig, 23°C) and CO_2/N_2 selectivity of 50–60 (White *et al.*, 2015; Xu *et al.*, 2019). In this paper, plate and frame modules of membrane unit with 1500 GPU and 30 CO_2/N_2 selectivity was applied. As shown in Fig. 3, the CO_2 recovery rate and desired membrane area of $CO_2/N_2/H_2O$, the mass transfer model of separation membrane was built in Aspen Plus calculator. The selectivity of CO_2/H_2O was set as 1, so the permeability coefficient of H_2O was identical with that of CO_2. The CO_2 concentration had been elevated to more than 20 vol% in the permeate gas.

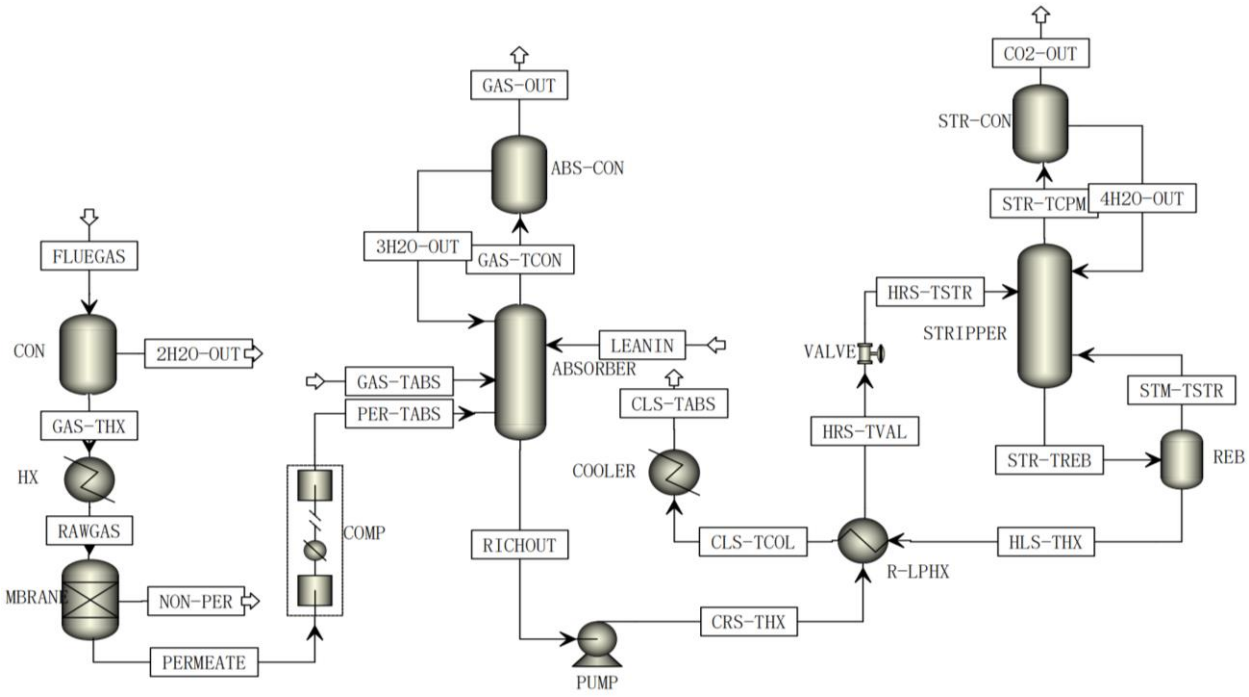

Fig. 2. Hybrid membrane-absorption process of CO_2 capture.

Table 2. Settings in the rate-based calculation.

Item	Absorber	Stripper
Packing type	Mellapak 250.Y	Mellapak 500.Y
Packing height	30 m	10 m
Column diameter	2.2 m	1.4 m
Flow model	Mixed model	Mixed model
Film resistance	Discrxn for liquid, film for vapor	
Interfacial area method	Bravo (1992)	

https://doi.org/10.4209/aaqr.2020.07.0374

Design specification $\theta_i = \frac{y_{iP}U_P}{x_{iF}U_F}$			
Recovery	θ_{CO2F}	0.2500	-
	θ_{H2OF}	0.2800	-
	θ_{N2F}	0.0270	-

CO2	1500	GPU
$\alpha_{CO2/N2}$	30	-
$\alpha_{CO2/H2O}$	1	-

Variate	Flue gas		Non-permeate gas		Permeate gas		Units
Flow	U_F	1341.288	U_R	1277.0545	U_p	52.49475	*kmol/h*
Pressure	P_F	106	P_R	106	p	10	*Kpa*
Composition	x_{CO2F}	0.030238	x_{CO2R}	0.0238191	y_{CO2p}	0.193151	-
	x_{H2OF}	0.022256	x_{H2OR}	0.0168305	y_{H2Op}	0.159226	-
	x_{N2F}	0.938754	x_{N2R}	0.9593504	y_{N2p}	0.647622	-
$\theta_i = \frac{y_{iP}U_P}{x_{iF}U_F}$			$x_{CO2R}U_R$	30.418307	$y_{CO2p}U_p$	10.13944	*kmol/h*
$y_{CO2p} + y_{H2Op} + y_{N2p} = 1$			$x_{H2OR}U_R$	21.493416	$y_{H2Op}U_p$	8.358551	*kmol/h*
$x_{iF}U_F = x_{iR}U_R + y_{iP}U_P$			$y_{N2p}U_R$	1225.1428	$y_{N2p}U_p$	33.99677	*kmol/h*
$x_{CO2R} + x_{H2OR} + x_{N2R} = 1$			U_R	1277.0545	U_p	52.49475	*kmol/h*

Average partial pressure difference			
$\overline{xP - yp_{CO2}}$	0.933508	kPa	$\overline{xP - yp_i} = x_i P - y_{ip} p$
$\overline{xP - yp_{H2O}}$	0.766892	kPa	
$\overline{xP - yp_{N_2}}$	93.03168	kPa	
Plate separation membrane			
Permeability coefficient	J_{CO2}	1.80E-03	kmol/(h·m²·kPa)
	J_{H2O}	1.80E-03	kmol/(h·m²·kPa)
	J_{N2}	6.00E-05	kmol/(h·m²·kPa)
A_{mCO2}	6034.25	$A_{mi} = \frac{y_{iP}U_P}{J_i(\overline{xP - yp_i})}$	
A_{mH2O}	6055.14	$\theta_i = \frac{J_i(\overline{xP - yp_i})A_m}{x_{iF}U_F}$	
A_{mN2}	6090.54		

Fig. 3. Mass *transfer* model of CO_2/N_2 separation membrane in Aspen Plus calculator.

3 RESULTS AND DISCUSSION

3.1 Structured Packing

The structured packing, as the core part of mass and heat transfer in the absorber, which determined the gas-solution flow mode and mass transfer coefficient. The structural parameter of the structured packing directly affected the absorption performance, such as absorber diameter, pressure drop of the structured packing section, rich CO_2 loading, solution flow and solution regeneration duty. According to the two-film mass transfer theory, the mass transfer process was theoretically controlled by Henry constant of gas physical dissolution in the CO_2-MEA absorption process. In the solution phase, the effect of gas-liquid reaction was expressed by the chemical enhancement factor $E = k_L/k_L^0$. The total mass transfer coefficient in the absorber with the reaction between CO_2 and amine solution was as follows:

$$K_G a_e = a_e \cdot \frac{Ek_L}{He} = a_e \cdot \frac{\sqrt{k_2[MEA]D_{CO_2,l}}}{He} \tag{3}$$

The gas-liquid reaction of the lower part of the absorber was controlled by the thermodynamic, while upper part was controlled by the dynamics. As a result, the reaction rate increased first and then decreased along with the structured packing height. For the NGCC power plant, the CO_2 partial pressure of the flue gas was low (about 4.0 vol%), the driving force of the reaction of the lower part of absorber was weak. In order to achieve 90% of the capture rate from the flue gas in NGCC power plant, higher specific surface area of the structured packing was needed. Fig. 4 showed the effect of packing height on flooding point and rich CO_2 loading. As the height of structured packing increased, the effective gas-liquid mass transfer area expanded, the gas-liquid contact time extended, the rich solution CO_2 loading increased, and the solution flow rate decreased. When the height of structured packing 250.Y ranged from 16 m to 30 m, the rich solution CO_2 loading increased from 0.294 to 0.396 mol-CO_2 mol-MEA^{-1}, and the flooding point reduced to 60.9% simultaneously.

The rich CO_2 loading and solution flow affected the latent heat of the CO_2 product gas which out from the stripper and sensible heat of the hot rich/lean solution in the regeneration process, which directly affected the regeneration duty. As shown in Fig. 5, the regeneration duty decreased with the increasing of the structured packing height. The results demonstrated that

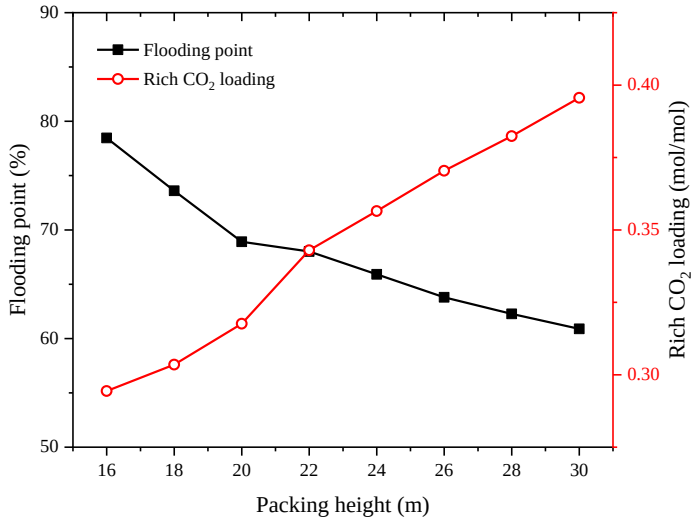

Fig. 4. Effect of packing height on rich CO_2 loading and flooding point of absorber.

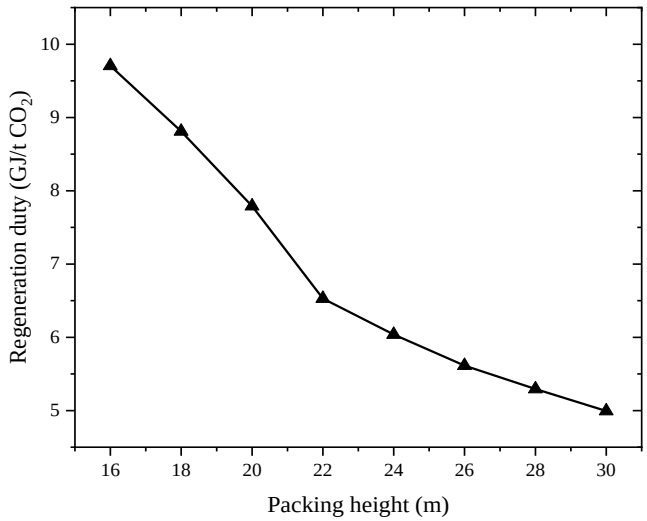

Fig. 5. Effect of packing height on solvent regeneration duty.

the optimal parameters selected were 90% CO_2 capture rate, 30 m 250.Y structured packing, 0.26 mol-CO_2 mol-MEA^{-1} lean CO_2 loading and 2.0 bar stripper pressure. Under this operating condition, the rich CO_2 loading and solvent regeneration duty were 0.396 mol-CO_2 mol-MEA^{-1} and 4.99 GJ t-CO_2^{-1}, respectively. The regeneration duty can be reduced to 4.54 GJ t-CO_2^{-1} when the total packing volume of 25 m IMTP 40 random packing was about 1.27 times of the 30 m 250.Y structured packing in the absorber (Luo *et al.*, 2015).

3.2 Flue Gas Inlet Stage

The reaction of the lower part of the absorber was controlled by thermodynamics. In order to increase the rich CO_2 loading, the permeate gas with higher CO_2 partial pressure should be pumped into the lower part of the absorber (Stage 20, 0 m packing location). The flue gas with low CO_2 partial pressure will affect this absorption process, so the inlet location should be discussed detailed at first. Fig. 6 showed the effect of inlet location on the rich CO_2 loading and solution regeneration duty. With the increasing of the number of flue gas inlet stage, the rich CO_2 loading increased first and then decreased. Overall, permeate gas with higher CO_2 partial pressure improved the driving force of the lower part of the absorber. Compared with traditional chemical absorption process, the higher rich CO_2 loading which resulting the lower solution flow and solution regeneration duty. When the inlet stage of flue gas with lower CO_2 pressure was

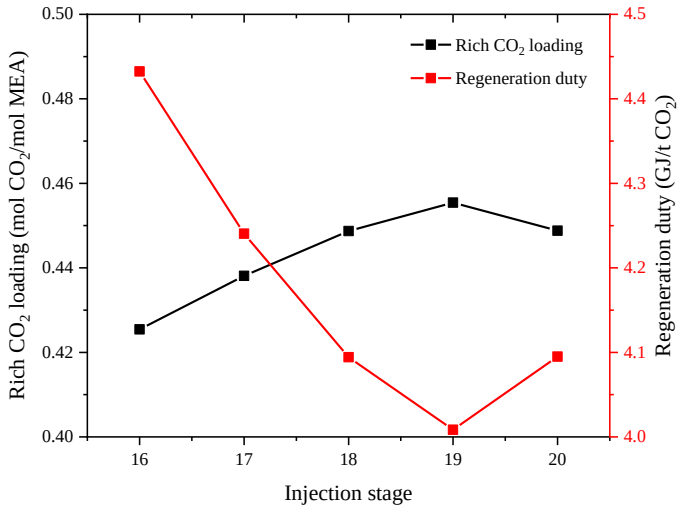

Fig. 6. Effect of flue gas inlet stage on rich CO_2 loading and solvent regeneration duty.

over Stage 19 (1.5 m packing location), the rich CO_2 loading will be reduced, and the regeneration energy consumption will increase sharply due to the mixture of flue gas with lower CO_2 partial pressure and permeate gas with higher CO_2 concentration. The optimal inlet stage of the absorber: Stage 18 (1.5 m packing location). The rich CO_2 loading was 0.455 mol-CO_2 mol-MEA^{-1}, and the minimum regeneration energy consumption was 4.01 GJ t-CO_2^{-1} under this operating condition. In this study, Stage 19 was selected as the inlet stage of the flue gas with low CO_2 partial pressure.

3.3 CO_2 Recovery Rate of Membrane Unit

The CO_2 recovery rate of the flue gas directly affected the permeated CO_2 concentration and membrane area, and then affected the rich CO_2 loading, solvent flow and regeneration duty of the hybrid membrane-absorption process. Therefore, it is necessary to study the effect of CO_2 recovery on the absorption process. As shown in Fig. 7, the permeate gas decreased slightly from 32.3 vol% to 28.7 vol% with increasing of flue gas CO_2 recovery rate (5–30%). The total cost of the hybrid amine-membrane system is lowest at 12% absorber inlet CO_2, and the flue gas split ratio was calculated by CHEMCAD (Ding *et al.*, 2017), while the actual CO_2 concentration of the permeate gas was higher than the value which calculated by CHEMCAD. The non-permeate gas CO_2 concentration had not changed much. The rich CO_2 loading increased with increasing of CO_2 recovery rate, which still far away from the saturation state. When the CO_2 recovery rate was over 20%, the rich CO_2 loading had not changed much. The total CO_2 capture capacity improved with the increasing of CO_2 recovery rate, while the solution flow did not change much.

As shown in Fig. 8, the average differential pressure of feed/permeate gas and the membrane area showed an approximate linear correlation with CO_2 recovery rate. The membrane unit operated under atmospheric conditions due to the vacuum compressor. The average differential pressure of the membrane unit as low as 1.2–1.42 kPa on this account.

For hybrid membrane-absorption process, the compressor power should be taken into account. The compressor power was linearly relative to the CO_2 recovery rate. The total regeneration duty included compressor power and solution regeneration duty. The total regeneration duty decreased first and then increased with the increasing of flue gas CO_2 recovery rate. As shown in Fig. 9, the total regeneration duty ranged from 3.81–4.12 GJ t-CO_2^{-1} when the CO_2 recovery rate ranged from 5% to 30%. The CO_2 capture scale increased with the increasing of CO_2 recovery of the flue gas. Considering the membrane area (membrane unit investment) and solvent flow, the optimal CO_2 recovery rate was selected as 20%.

The permeate gas with high CO_2 concentration was pumped into the absorber on Stage 20, and the flue gas with low CO_2 concentration inlet position was set as Stage 19. In such operating condition, these two gases will be inevitably mixed at the position on Stage 18. From Fig. 10, it can be seen that the concentration of flue gas CO_2 changed sharply on Stages 18–20 in the

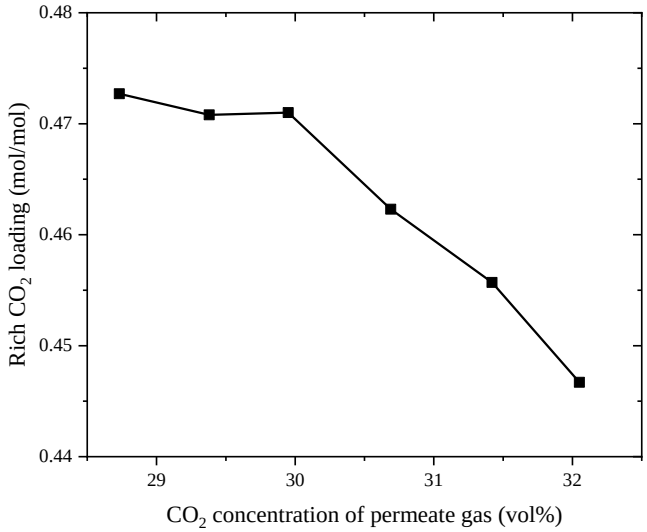

Fig. 7. Effect of CO_2 recovery rate on rich CO_2 loading.

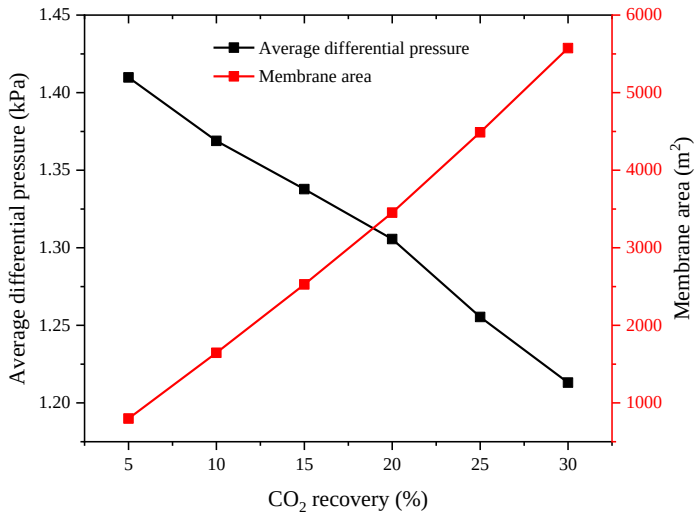

Fig. 8. Average differential pressure and membrane area.

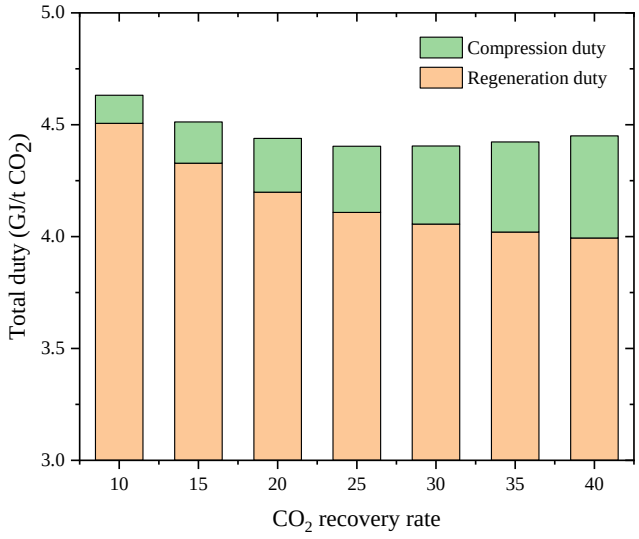

Fig. 9. Effect of CO_2 recovery rate on total duty.

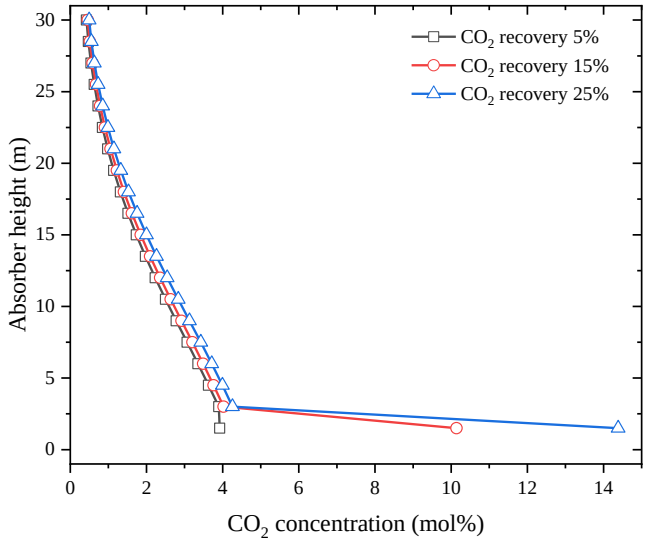

Fig. 10. CO_2 concentration profile of absorber column.

absorber. The CO_2 concentration dropped to about 4.0 vol% on Stage 19, so it was considered that the two gases were completely mixed at this position.

3.4 Flue Gas Flow of Membrane Unit

In order to reduce the compressor power, vacuum compressor was applied in the hybrid process. To improve the CO_2 capture rate of the hybrid membrane-absorption process, the flue gas flow of membrane unit should be optimized. At first, the flow of flue gas in membrane unit was equal to the flow in absorber column. Fig. 11 showed CO_2 concentration of permeate gas and rich CO_2 loading under different flue gas flow (30~100%). Under this condition, CO_2 concentration reduced from 29.95% to 23.40%. The permeate gas with higher CO_2 partial pressure will improve the driving force at the bottom of absorber, so the lower CO_2 partial pressure will result in lower rich CO_2 loading. CO_2 concentration of permeate gas had less effect on the rich CO_2 loading and solution regeneration duty. The increasing of permeate gas flow which resulting in higher compressor power due to the decreasing CO_2 concentration of permeate gas. However, the compressor power occupied a small portion in total regeneration duty.

According to Eq. (1), the required membrane area had a significant linear correlation with the average partial difference between feed and permeate gas. Fig. 12 showed the average differential pressure and membrane area ratio under different flow ratio. The membrane area increased rapidly when the flow ratio was over 50%. When the flue gas flow ratio in membrane unit was 30%, the average partial pressure difference decreased by 40%, and membrane area increased by 43.67%. The optimal flow ratio was selected as 50%, and the required membrane area was about 115% of 100% flow ratio condition.

3.5 Pressure Ratio between Feed and Permeate Gas

To reduce the power of vacuum compressor, increasing of membrane area and decreasing of pressure difference between two sides of the membrane can be applied. While the membrane area and permeate side pressure will affect the investment cost and operating cost, these two parameters should be optimized. Table 3 showed the membrane separation, absorption and regeneration performance under different flow and pressure difference ratio. When the pressure difference ratio was 5:1. The process had lower rich CO_2 loading, higher compressor power and solvent regeneration duty under lower pressure difference ratio. CO_2 concentration of permeate gas dropped to 16.95–28.60 vol%. The compressor power increased would rise by 10% due to greater permeate gas flow. The total regeneration duty of 5:1 pressure difference ratio increases of 2.64–3.59% compared with 10:1 pressure difference ratio. And even worse is that the membrane area was double. The optimal total regeneration duty was reduced by 20.7% when flow ratio and CO_2 recovery were 100% and 20% respectively.

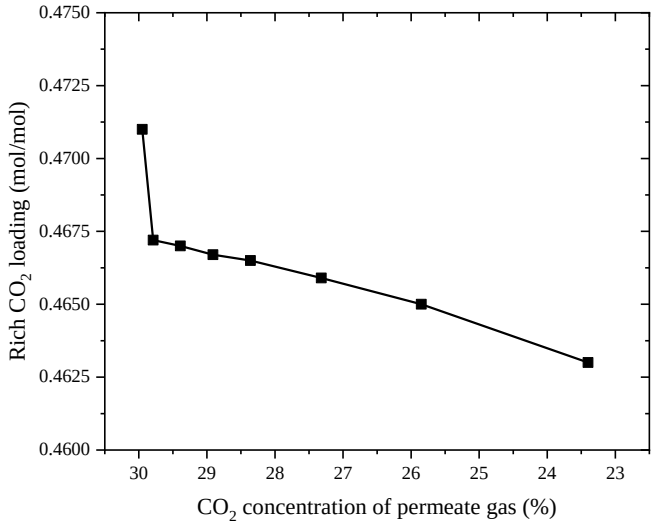

Fig. 11. CO_2 concentration of permeate gas and rich CO_2 loading.

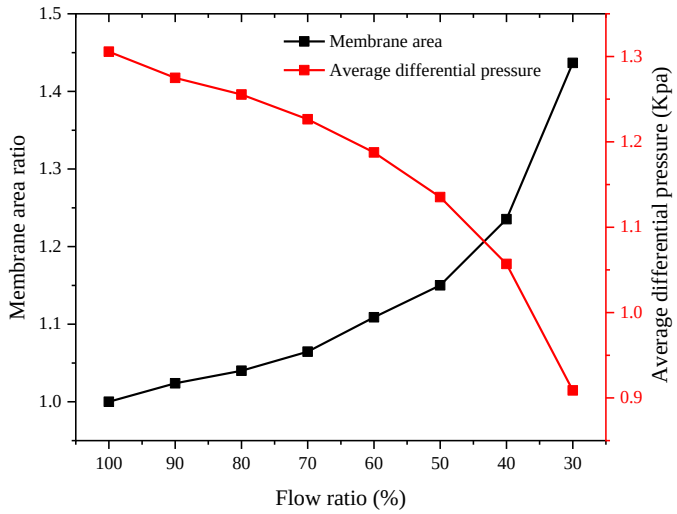

Fig. 12. Effect of flow ratio on average differential pressure and membrane area ratio.

Table 3. Membrane and absorption performance under different pressure ratio.

Flow ratio %	CO_2 recovery %	Pres. ratio –	Per CO_2 vol%	RLD mol/mol	A_{mem} m^2	Q_{comp} GJ t-CO_2^{-1}	Q_{reb} GJ t-CO_2^{-1}
100	20	10:1	29.95	0.471	3452.57	0.1318	3.825
100	20	5:1	18.60	0.460	7293.44	0.1455	3.950
50	40	10:1	27.32	0.466	3970.73	0.1446	3.882
50	40	5:1	16.95	0.458	8255.99	0.1598	3.973

4 CONCLUSIONS

The chemical absorption process for capturing CO_2 is influenced by the CO_2 concentration of the permeating gas, the area of the membrane and the power of the compressor. Hence, we developed an integrated mass transfer model of a separating membrane in Aspen Plus that simulated the flow, composition and pressure of the permeating gas as well as the required area for the membrane. To improve the driving force of the gas-liquid equilibrium, flue gas with a low CO_2 concentration was pumped into the absorber on Stage 19, which increased the CO_2 load in

the MEA from 0.396 to 0.471 mol-CO_2 mol-MEA^{-1}. Using a lower feed-gas-to-permeating-side-gas pressure ratio degraded the separation performance, with a lower CO_2 concentration in the permeating gas, a lower CO_2 load in the MEA, higher power consumption by the compressor and a higher heat duty for the solvent regeneration. The required area for the membrane primarily depended on the ratio of the feed gas pressure to the permeating-side gas pressure and the flow rate of the flue gas, more than doubling in size when these two parameters were reduced. The optimal feed-gas-to-permeating-side-gas pressure ratio and the flue gas flow rate were found to be 10:1 and 50%, respectively. Furthermore, compared to traditional chemical absorption, the solvent regeneration's heat duty decreased by more than 20.7% when the gas flow rate and the CO_2 recovery rate were 100% and 20%, respectively.

REFERENCES

Agbonghae, E.O., Hughes, K.J., Ingham, D.B., Ma, L., Pourkashanian, M. (2014). Optimal process design of commercial-scale amine-based CO_2 capture plants. Ind. Eng. Chem. Res. 53, 14815–14829. https://doi.org/10.1021/ie5023767

Ahn, H., Luberti, M., Liu, Z., Brandani, S. (2013). Process configuration studies of the amine capture process for coal-fired power plants. Int. J. Greenhouse Gas Control. 16, 29–40. https://doi.org/10.1016/j.ijggc.2013.03.002

Akram, M., Ali, U., Best, T., Blakey, S., Finney, K.N., Pourkashanian, M. (2016). Performance evaluation of PACT pilot-plant for CO_2 capture from gas turbines with exhaust gas recycle. Int. J. Greenhouse Gas Control. 47, 137–150. https://doi.org/10.1016/j.ijggc.2016.01.047

Amann, J.M.G and Bouallou, C. (2009). CO_2 capture from power stations running with natural gas (NGCC) and pulverized coal (PC): Assessment of a new chemical solvent based on aqueous solutions of N-MethylDiEthanolAmine + TriEthylene TetrAmine. Energy Procedia 1, 909–916. https://doi.org/10.1016/j.egypro.2009.01.121

Artanto, Y., Jansen, J., Pearson, P., Do, T., Cottrell, A., Meuleman, E., Feron, P. (2012). Performance of MEA and amine-blends in CSIRO PCC pilot plant at loy yang power in Australia. Fuel 101, 264-275. https://doi.org/10.1016/j.fuel.2012.02.023

Ding, J., Freeman, B., Rochelle, G.T. (2017). Regeneration design for NGCC CO_2 capture with amine-only and hybrid amine/membrane. Energy Procedia 114, 1394–1408. https://doi.org/10.1016/j.egypro.2017.03.1264

Freeman, B., Hao, P., Baker, R., Kniep, J., Chen, E., Ding, J., Zhang, Y., Rochelle, G.T. (2014). Hybrid membrane-absorption CO_2 capture process. Energy Procedia 63, 605–613. https://doi.org/10.1016/j.egypro.2014.11.065

Frimpong, R.A., Irvin, B.D., Nikolic, H., Liu, K., Figueroa, J. (2019). Integrated hybrid process for solvent-based CO_2 capture using a pre-concentrating membrane: A pilot scale study. Int. J. Greenhouse Gas Control. 82, 204–209. https://doi.org/10.1016/j.ijggc.2019.01.016

Le Moullec, Y., Kanniche, M. (2011). Screening of flowsheet modifications for an efficient monoethanolamine (MEA) based post-combustion CO_2 capture. Int. J. Greenhouse Gas Control. 5, 727–740. https://doi.org/10.1016/j.ijggc.2011.03.004

Li, H., Ditaranto, M., Berstad, D. (2011). Technologies for increasing CO_2 concentration in exhaust gas from natural gas-fired power production with post-combustion, amine-based CO_2 capture. Energy 36, 1124–1133. https://doi.org/10.1016/j.energy.2010.11.037

Liu, B., Yang, X., Wang, T., Zhang, M., Chiang, P.C. (2019). CO_2 separation by using a three-stage membrane process. Aerosol Air Qual. Res. 19, 2917–2928. https://doi.org/10.4209/aaqr.2019.10.0519

Liu, F., Fang, M., Yi, N., Wang, T. (2019). Research on alkanolamine-based physical-chemical solutions as biphasic solvents for CO_2 capture. Energy Fuels 33, 11389–11398. https://doi.org/10.1021/acs.energyfuels.9b02392

Luo, X., Wang, M., Chen, J. (2015). Heat integration of natural gas combined cycle power plant integrated with post-combustion CO_2 capture and compression. Fuel 151, 110–117. https://doi.org/10.1016/j.fuel.2015.01.030

Luo, X., and Wang, M. (2016). Optimal operation of MEA-based post-combustion carbon capture for natural gas combined cycle power plants under different market conditions. Int. J.

Greenhouse Gas Control. 48, 312–320. https://doi.org/10.1016/j.ijggc.2015.11.014

Mangalapally, H.P., Notz, R., Asprion, N., Sieder, G., Garcia, H., Hase, H. (2012). Pilot plant study of four new solvents for post combustion carbon dioxide capture by reactive absorption and comparison to MEA. Int. J. Greenhouse Gas Control. 8, 205–216. https://doi.org/10.1016/j.ijggc.2012.02.014

Martín-Gamboa, M., Iribarren, D., Dufour, J. (2018). Environmental impact efficiency of natural gas combined cycle power plants: A combined life cycle assessment and dynamic data envelopment analysis approach. Sci. Total Environ. 615, 29–37. https://doi.org/10.1016/j.scitotenv.2017.09.243

Mores, P.L., Godoy, E., Mussati, S.F., Scenna, N.J. (2014). A NGCC power plant with a CO_2 post-combustion capture option. Optimal economics for different generation/capture goals. Chem. Eng. Res. Des. 92, 1329–1352. https://doi.org/10.1016/j.cherd.2013.11.013

Mubashir, M., Fong, Y.Y., Leng, C.T., Keong, L.K. (2018). Issues and current trends of hollow-fiber mixed-matrix membranes for CO_2 separation from N_2 and CH_4. Chem. Eng. Technol. 41, 235–252. https://doi.org/10.1002/ceat.201700327

Notz, R., Mangalapally, H.P., Hasse, H. (2012). Post combustion CO_2 capture by reactive absorption: Pilot plant description and results of systematic studies with MEA. Int. J. Greenhouse Gas Control. 6, 84–112. https://doi.org/10.1016/j.ijggc.2011.11.004

Oh, S.Y., Binns, M., Cho, H., Kim, J.K. (2016). Energy minimization of MEA-based CO_2 capture process. Appl. Energy 169, 353–362. https://doi.org/10.1016/j.apenergy.2016.02.046

Rabensteiner, M., Kinger, G., Koller, M., Gronald, G., Hochenauer, C. (2014). Pilot plant study of ethylenediamine as a solvent for post combustion carbon dioxide capture and comparison to monoethanolamine. Int. J. Greenhouse Gas Control. 27, 1–14. https://doi.org/10.1016/j.ijggc.2014.05.002

von Harbou, I., Mangalapally, H.P., Hasse, H. (2013). Pilot plant experiments for two new amine solvents for post-combustion carbon dioxide capture. Int. J. Greenhouse Gas Control. 18, 305–314. https://doi.org/10.1016/j.ijggc.2013.08.002

White, L.S., Wei, X.T., Pande, S., Wu, T., Merkel, T.C. (2015). Extended flue gas trials with a membrane-based pilot plant at a one-ton-per-day carbon capture rate. J. Membr. Sci. 496, 48–57. https://doi.org/10.1016/j.memsci.2015.08.003

Xu, J., Wang, Z., Qiao, Z., Wu, H., Dong, S., Zhao S., Wang J. (2019). Post-combustion CO_2 capture with membrane process: Practical membrane performance and appropriate pressure. J. Membr. Sci. 581, 195–213. https://doi.org/10.1016/j.memsci.2019.03.052

Yang, J., Yu, W., Wang, T., Liu, Z., Fang, M. (2020). Process simulations of the direct non-aqueous gas stripping process for CO_2 desorption. Ind. Eng. Chem. Res. 59, 7121–7129. https://doi.org/10.1021/acs.iecr.9b05378

Yu, C.H., Huang, C.H., Tan, C.S. (2012). A Review of CO_2 Capture by absorption and adsorption. Aerosol Air Qual. Res. 12, 745–769. https://doi.org/10.4209/aaqr.2012.05.0132

Yu, W., Wang T., Alissa Park, A.H., Fang, M. (2019). Review of liquid nano-absorbents for enhanced CO_2 capture. Nanoscale 11, 17137–17156. https://doi.org/10.1039/C9NR05089B

Yu, W., Wang, T., Alissa Park, A.H., Fang, M. (2020). Toward sustainable energy and materials: CO_2 capture using microencapsulated sorbents. Ind. Eng. Chem. Res. 59, 9746–9759. https://doi.org/10.1021/acs.iecr.0c01065